High-efficiency grating coupler for ultra-low loss Si_3N_4 based platform

B. CHMIELAK,[1] S. SUCKOW,[1] J. PARRA,[2] V. C. DUARTE,[3] T. MENGUAL,[3] M. A. PIQUERAS,[3] A. L. GIESECKE,[1] M. C. LEMME,[1,4] AND P. SANCHIS[2,*]

[1]*AMO GmbH, Otto-Blumenthal-Str. 25, 52074 Aachen, Germany*
[2]*Nanophotonics Technology Center, Universitat Politècnica de València, Camino de Vera s/n, 46022 Valencia, Spain*
[3]*DAS Photonics S.L., Camino de Vera s/n, 46022 Valencia, Spain*
[4]*Chair of Electronic Devices, RWTH Aachen University, Otto-Blumenthal-Str. 2, 52074 Aachen, Germany*
**Corresponding author: pabsanki@ntc.upv.es*

Received XX Month XXXX; revised XX Month, XXXX; accepted XX Month XXXX; posted XX Month XXXX (Doc. ID XXXXX); published XX Month XXXX

Integrated silicon nitride waveguides of 100 nm height can achieve ultra-low propagation losses below 0.1 dB/cm at the 1550 nm wavelength band but lack the scattering strength to form efficient grating couplers. An enhanced grating coupler design based on an amorphous silicon layer on top of the silicon nitride is proposed and demonstrated to improve the directionality of the coupler. The fabrication process is optimized for a self-alignment process between the amorphous silicon and silicon nitride layers without increasing waveguide losses. Experimental coupling losses of 5 dB and a 3 dB bandwidth of 75 nm are achieved with both regular and focusing designs.

Photonic technologies may provide multiple benefits in a wide range of application fields from telecom/datacom and new paradigms in high-performance computing to light detection and ranging (LiDAR) systems and space communications [1-5]. For many applications, photonics has the potential to provide a higher speed operation and lower energy consumption compared to solutions based on electronics. However, a key performance metric is often ensuring the lowest insertion losses. In fact, high losses imply that larger optical power budgets are required, which ultimately limits the energy consumption improvement that photonics may provide.

Insertion losses in photonic integrated circuits (PICs) are mainly dominated by the waveguide propagation losses and coupling losses to external optical fibers. Waveguide propagation losses are especially critical when waveguide lengths on the order of several centimeters are required. High-index contrast waveguides, such as silicon waveguides, achieve compact PIC footprints due to the high confinement of the optical mode in the waveguide core but propagation losses are highly sensitive to sidewall roughness. On the other hand, low-index contrast waveguides, such as SiO_2 waveguides, may provide much lower propagation losses due to the weaker mode confinement and, therefore smaller influence of Rayleigh scattering on sidewall roughness. A good trade-off to fulfill both requirements are silicon nitride (Si_3N_4) waveguides, which also have a relatively high-index contrast and are complementary metal–oxide–semiconductor (CMOS)-compatible [6].

Silicon nitride has gained a lot of interest in the last years for implementing PICs with lower propagation losses compared to silicon and a broader operational wavelength band that allows applications ranging from the visible to the mid-infrared. Furthermore, several approaches for high-efficiency coupling with grating couplers have also been reported [7-12]. For such approaches using ~400-nm-thick Si_3N_4 waveguides, the grating strength is moderate, and the directionality is usually improved by adding a bottom reflector [8,9,12], or by engineering the teeth geometry [10]. However, the implementation of efficient grating coupling approaches is more challenging in the case of ultra-low loss waveguides based on thin Si_3N_4 cores [13]. A relatively simple approach is to enhance the directionality of the grating through the deposition of a high refractive index material in the grating coupling area [14]. Such a concept has been demonstrated in grating couplers for silicon waveguides [15,16]. However, to the best of our knowledge, the application for Si_3N_4 waveguides is proposed for the first time in this work.

The paper is structured as follows. The proposed PIC platform based on thin Si_3N_4 photonic waveguides with ultra-low propagation losses below 0.1 dB/cm at 1550 nm wavelengths is first described. Then, the design, fabrication process, and characterization of high-efficiency grating

couplers made by depositing an amorphous silicon layer on top of the grating structure is addressed. Regular and focusing coupler designs are reported with experimental coupling losses of 5 dB, which significantly outperform the losses achieved by a standard grating design.

A cross-section of the proposed ultra-low loss single-mode Si_3N_4 photonic waveguide is shown in Fig. 1(a). The core consists of a 2.8 µm wide and 100 nm high stoichiometric Si_3N_4 waveguide, located on top of a 6 µm thick silicon dioxide (SiO_2) buffer layer that separates it from the silicon (Si) substrate. The waveguide core is covered by a 1.6 µm thick low-temperature oxide (LTO) cladding layer. The simulated mode profile for transverse electric (TE) polarization at 1550 nm wavelength is shown in Fig. 1(b).

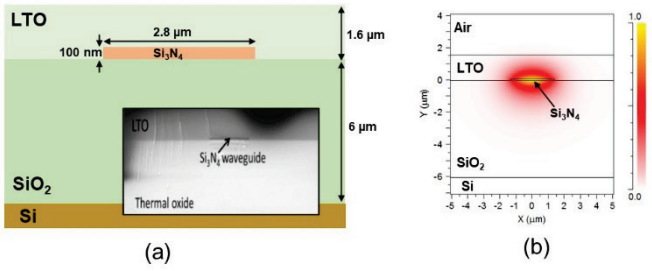

Fig. 1. (a) Cross-section of the ultra-low loss Si_3N_4 photonic waveguide and SEM image of the fabricated waveguide. (b) Simulated E_x electric field mode profile at 1550 nm.

The Si_3N_4 waveguide core was fabricated by low-pressure chemical vapor deposition (LPCVD). The waveguide layer is defined via optical projection lithography with an i-line stepper tool and patterned via reactive ion etching (RIE). An optimized RIE process is used, which yields steep and smooth sidewalls that are essential for low loss operation. After the etching step, the photoresist mask is removed using oxygen plasma, and subsequently, the LTO cladding material is deposited via LPCVD. Finally, the wafer is annealed at 1000°C for several hours, which is critical for improving the quality of the LTO layer and so ensuring low-loss operation. Indeed, any high-temperature deposition process of high-quality SiO_2 should provide low losses. A scanning electron microscopy (SEM) image of the fabricated waveguide is depicted as an inset in Fig. 1(a). The cut-back method with several waveguides of different length on the same chip was used to characterize the propagation losses. To achieve a good statistic, a full 6" wafer featuring photonic waveguides with varying lengths from 1.5 cm to 109 cm was fabricated and characterized thoroughly, yielding ultra-low propagation losses below 0.1 dB/cm (see Supplementary Material for more details).

Standard uniform grating couplers were first designed. The refractive indices of materials used for design are n_{Si}=3.48, n_{SiO2}=1.45, n_{Si3N4}=1.99, n_{LTO}=1.44. Due to the thin waveguide core, only full etching of the Si_3N_4 layer, as depicted in Fig. 2(a), is considered. However, high coupling losses around 12 dB and very low directionality (~13 %) are obtained for the best design with a grating period of 1.17 µm, a filling factor of 50%, and an incident optical fiber angle of 10º. Therefore, an enhanced approach is required to minimize this value.

The directionality of the grating coupler, and so the coupling efficiency, may be improved by depositing an additional material with a higher refractive index on top of the grating [17]. Following this approach, a new design was carried out for amorphous silicon (a-Si) as the high-index material. For amorphous silicon, the same index as silicon was considered. The enhanced grating structure is shown in Fig. 2(b). A scan of the optimum a-Si thickness and grating period was carried out by means of 2D-FDTD simulations [14], considering a filling factor of the grating of 50% and an incident optical fiber angle of 10º. The simulated coupling efficiency and reflectivity at 1550 nm wavelength are shown in Fig. 2(c) and 2(d), respectively.

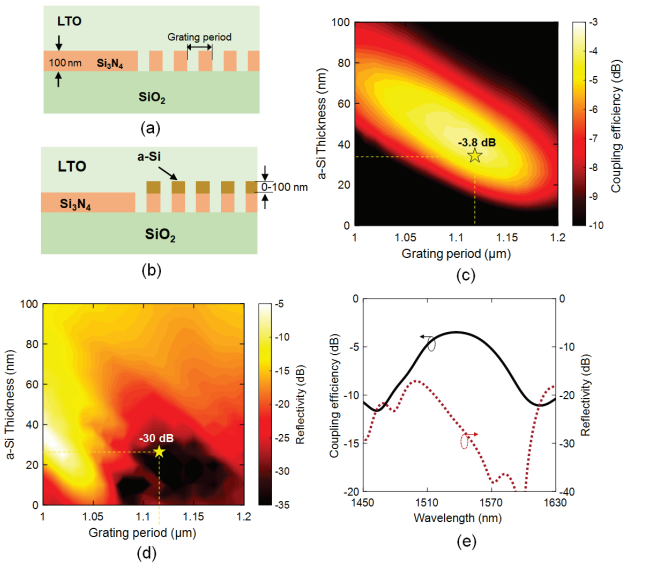

Fig. 2. (a) Standard uniform grating coupler and (b) enhanced design with a-Si layer on top. (c) Coupling efficiency and (d) reflectivity as a function of the a-Si thickness and grating period at λ = 1550 nm. (e) Simulated transmission and reflectivity spectra.

The optimum design is found for an amorphous silicon thickness of 35 nm and a grating period of 1.12 µm. The simulated coupling losses are significantly reduced to 3.8 dB, while reflectivity is close to -30 dB. The simulated spectra of coupling efficiency and reflectivity are depicted in Fig. 2(e). The coupling strength and coupling length of the grating are ~0.11 μm^{-1} and ~4.55 µm, according to our simulations. On the other hand, the directionality of the grating is ~53 %, which is a four-fold increase compared to the design without the a-Si layer. Figure 3 shows the field distribution at 1550 nm of the standard uniform grating coupler with the best performance and the enhanced design using the 35-nm-thick a-Si layer. For the standard version [Fig. 3(a)], only a small value of power is radiated due to the weak diffraction strength

of the grating. By opposite, including the a-Si layer significantly improves the directionality of the grating in the enhanced version, as shown in Fig. 3(b).

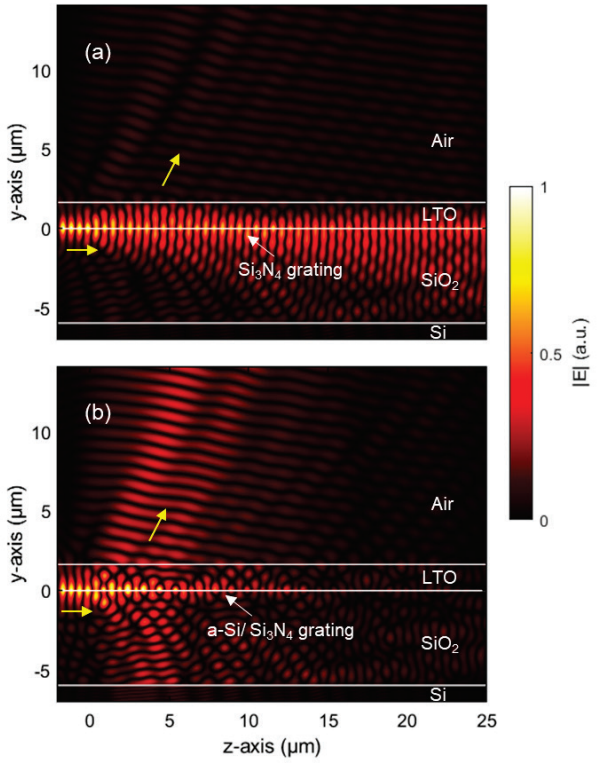

Fig. 3. Field distribution of (a) standard uniform grating coupler with optimum period and (b) enhanced grating coupler with 35-nm-thick a-Si layer. Results are given at λ = 1550 nm.

The fabrication process was adapted to allow the fabrication of the enhanced grating coupler design. The fabrication steps are summarized in Fig. 4(a). A 35 nm thick a-Si layer was deposited by sputtering on top of the Si_3N_4 layer before patterning both layers in one RIE step using a standard photoresist mask. Thereby a perfect alignment between a-Si and Si_3N_4 stripes is achieved inside the grating. The etching time was controlled using an endpoint detection system that analyzes the plasma spectrum and indicates when a layer is completely etched. Next, the a-Si layer had to be selectively removed from the Si_3N_4 waveguides while protecting it on the grating. For this purpose, the grating area was covered with a resist mask, as shown in Fig. 4(b). Subsequently, the a-Si was removed by wet chemical etching and using a silicon etch solution (mixture of different acids) to avoid damaging the Si_3N_4 waveguide and so keeping the ultra-low propagation losses (see Supplementary Material for more details). Figure 4(c) shows a SEM image of the fabricated grating after this step. The etching rate of Si_3N_4 was measured to be approx. 0.1 nm/min, while for the a-Si it was approximately 20 nm/min. After resist removal, the fabrication continued with the LTO deposition and the final annealing step. The a-Si is expected to become nano-crystalline during this annealing, but the refractive index remains very close to the index of a-Si so that any a-Si crystallization is expected to have a negligible influence on the grating coupler performance.

Input and output grating couplers were connected to 2 mm long straight waveguides by using a linear taper structure with 475 µm length. Light was injected from a tunable broadband laser, and an external fiber polarization controller was used to adjust the polarization to TE. A cleaved optical fiber was placed above the input grating at 10° with respect to the vertical axis to couple the TE polarized light into the chip. At the output, the same scheme was used to extract the light from the chip and measure the optical power by means of an optical power meter. Figure 5 shows the experimental coupling efficiency as a function of wavelength. Coupling losses of 5 dB were achieved, which is reasonably close to the simulated value. Furthermore, a 3 dB optical bandwidth of 75 nm was measured, being also in very good agreement with simulations.

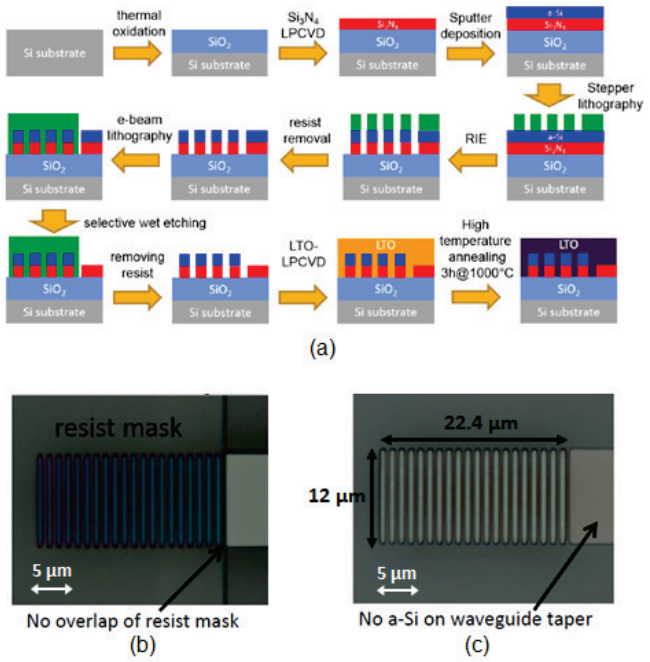

Fig. 4. (a) Description of fabrication process steps to include the enhanced grating couplers in the ultra-low loss waveguide platform. (b) SEM image of the grating coupler with resist mask for removing the a-Si layer from the waveguide and (c) SEM image after the etching process. The grating has 20 periods of length (22.4 µm) and a width of 12 µm.

A focusing grating coupler design with a 30 µm long taper between the grating coupler and waveguide was also carried out to save die area compared to the initially used 475 µm long taper. The grating coupler structure has the same design parameters as the regular one, and it was fabricated with the same fabrication process. The inset of Fig. 5 shows a SEM image of the focusing grating. The measured transmission spectrum is almost identical to the ones of the regular gratings, as can be seen in Fig. 5, but the footprint of the overall coupling structure is significantly reduced.

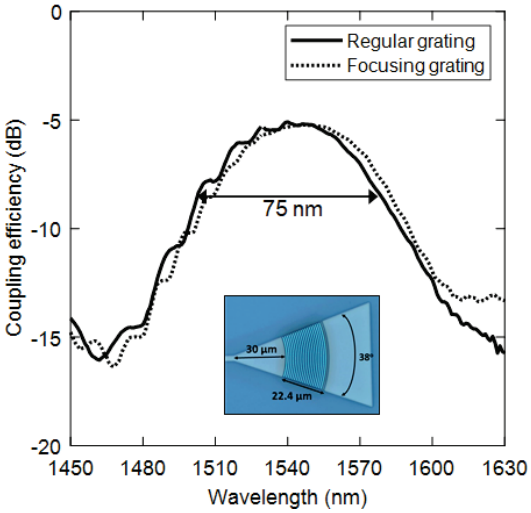

Fig. 5. Experimental coupling efficiency as a function of wavelength for the regular and focusing designs. The 3 dB optical bandwidth is 75 nm. An optical image of the fabricated focusing grating is depicted in the inset.

In summary, an enhanced grating coupler structure for efficient coupling into ultra-low loss Si_3N_4 photonic waveguides has been proposed and experimentally demonstrated. Coupling losses have been minimized by adding a thin amorphous silicon layer on top of the Si_3N_4 to improve the directionality of the grating. The fabrication process has been optimized to achieve a self-alignment process between the a-Si and Si_3N_4 layers that form the grating. Experimental coupling losses of 5 dB have been demonstrated, which significantly improve the 12 dB losses achieved by an optimized regular grating. Furthermore, a focusing design has also been demonstrated to reduce the coupler footprint.

Funding. EU-funded H2020 project RETINA (grant agreement n° 821943).

Disclosures. The authors declare no conflicts of interest.

Data availability. Data underlying the results presented in this paper are not publicly available at this time but may be obtained from the authors upon reasonable request.

Supplemental document. See Supplementary Material for supporting content on the waveguide propagation losses.

References

1. P. J. Winzer, D. T. Neilson, and A. R. Chraplyvy, Opt. Express 26, 24190 (2018).
2. B. J. Shastri, A. N. Tait, T. Ferreira de Lima, W. H. P. Pernice, H. Bhaskaran, C. D. Wright, and P. R. Prucnal, Nat. Photonics 15, 102–114 (2021).
3. J. Wang, F. Sciarrino, A. Laing, and M. G. Thompson, Nat. Photonics (2019).
4. J.-W. Shi, J.-I. Guo, M. Kagami, P. Suni, and O. Ziemann, Opt. Express 27, 7627 (2019).
5. C. Ciminelli, F. Dell'Olio and M. N. Armenise, World Scientific, 2016.
6. D. J. Blumenthal, R. Heideman, D. Geuzebroek, A. Leinse, and C. Roeloffzen, Proc. IEEE 106, 2209–2231 (2018).
7. C. R. Doerr, L. Chen, Y. K. Chen, and L. L. Buhl, IEEE Photonics Technol. Lett. 22, 1461–1463 (2010).
8. H. Zhang, C. Li, X. Tu, J. Song, H. Zhou, X. Luo, Y. Huang, M. Yu, and G. Q. Lo, Opt. Express 22, 21800 (2014).
9. J. Zou, Y. Yu, M. Ye, L. Liu, S. Deng, and X. Zhang, Opt. Express 23, 26305 (2015).
10. Y. Chen, R. Halir, Í. Molina-Fernández, P. Cheben, and J.-J. He, Opt. Lett. 41, 5059 (2016).
11. E. W. Ong, N. M. Fahrenkopf, and D. D. Coolbaugh, OSA Contin. 1, 13 (2018).
12. J. Hong, A. M. Spring, F. Qiu, and S. Yokoyama, Sci. Rep. 9, 1–8 (2019).
13. J. F. Bauters, M. J. R. Heck, D. John, D. Dai, M.-C. Tien, J. S. Barton, A. Leinse, R. G. Heideman, D. J. Blumenthal, and J. E. Bowers, Opt. Express 19, 3163-3174 (2011).
14. R. Marchetti, C. Lacava, L. Carroll, K. Gradkowski, and P. Minzioni, Photonics Res. 7, 201 (2019).
15. G. Roelkens, D. Van Thourhout, and R. Baets, Opt. Express 14, 11622–11630 (2006).
16. D. Vermeulen, S. Selvaraja, P. Verheyen, G. Lepage, W. Bogaerts, P. Absil, D. Van Thourhout, and G. Roelkens, Opt. Express 18, 18278–18283 (2010).
17. Synopsys, RSoft package. Available: https://www.synopsys.com/photonic-solutions.html

References with title

1. P. J. Winzer, D. T. Neilson, and A. R. Chraplyvy, "Fiber-optic transmission and networking: the previous 20 and the next 20 years [Invited]," Opt. Express 26, 24190 (2018).
2. B. J. Shastri, A. N. Tait, T. Ferreira de Lima, W. H. P. Pernice, H. Bhaskaran, C. D. Wright, and P. R. Prucnal, "Photonics for artificial intelligence and neuromorphic computing," Nat. Photonics 15, 102–114 (2021).
3. J. Wang, F. Sciarrino, A. Laing, and M. G. Thompson, "Integrated photonic quantum technologies," Nat. Photonics (2019).
4. J.-W. Shi, J.-I. Guo, M. Kagami, P. Suni, and O. Ziemann, "Photonic technologies for autonomous cars: feature introduction," Opt. Express 27, 7627 (2019).
5. C. Ciminelli, F. Dell'Olio and M. N. Armenise, "Photonics in Space: Advanced Photonic Devices and Systems", World Scientific, 2016.
6. D. J. Blumenthal, R. Heideman, D. Geuzebroek, A. Leinse, and C. Roeloffzen, "Silicon Nitride in Silicon Photonics," Proc. IEEE 106, 2209–2231 (2018).
7. C. R. Doerr, L. Chen, Y. K. Chen, and L. L. Buhl, "Wide bandwidth silicon nitride grating coupler," IEEE Photonics Technol. Lett. 22, 1461–1463 (2010).
8. H. Zhang, C. Li, X. Tu, J. Song, H. Zhou, X. Luo, Y. Huang, M. Yu, and G. Q. Lo, "Efficient silicon nitride grating coupler with distributed Bragg reflectors," Opt. Express 22, 21800 (2014).
9. J. Zou, Y. Yu, M. Ye, L. Liu, S. Deng, and X. Zhang, "Ultra efficient silicon nitride grating coupler with bottom grating reflector," Opt. Express 23, 26305 (2015).
10. Y. Chen, R. Halir, Í. Molina-Fernández, P. Cheben, and J.-J. He, "High-efficiency apodized-imaging chip-fiber grating coupler for silicon nitride waveguides," Opt. Lett. 41, 5059 (2016).
11. E. W. Ong, N. M. Fahrenkopf, and D. D. Coolbaugh, " SiNx bilayer grating coupler for photonic systems," OSA Contin. 1, 13 (2018).
12. J. Hong, A. M. Spring, F. Qiu, and S. Yokoyama, "A high efficiency silicon nitride waveguide grating coupler with a multilayer bottom reflector," Sci. Rep. 9, 1–8 (2019).
13. J. F. Bauters, M. J. R. Heck, D. John, D. Dai, M.-C. Tien, J. S. Barton, A. Leinse, R. G. Heideman, D. J. Blumenthal, and J. E. Bowers, "Ultra-low-loss high-aspect-ratio Si_3N_4 waveguides," Opt. Express 19, 3163-3174 (2011).
14. R. Marchetti, C. Lacava, L. Carroll, K. Gradkowski, and P. Minzioni, "Coupling strategies for silicon photonics integrated chips [Invited]," Photonics Res. 7, 201 (2019).
15. G. Roelkens, D. Van Thourhout, and R. Baets, "High efficiency silicon-on-insulator grating coupler based on a poly-silicon overlay," Opt. Express 14, 11622–11630 (2006).
16. D. Vermeulen, S. Selvaraja, P. Verheyen, G. Lepage, W. Bogaerts, P. Absil, D. Van Thourhout, and G. Roelkens, "High-efficiency fiber-to-chip grating couplers realized using an advanced CMOS-compatible silicon-on-insulator platform," Opt. Express 18, 18278–18283 (2010).
17. Synopsys, RSoft package. Available: https://www.synopsys.com/photonic-solutions.html